Contract No:

This document was prepared in conjunction with work accomplished under Contract No. DE-AC09-08SR22470 with the U.S. Department of Energy (DOE) Office of Environmental Management (EM).

Disclaimer:

COMPACT CRYO-ADSORBENT HYDROGEN STORAGE SYSTEMS FOR FUEL CELL VEHICLES

Dr. David Tamburello
Savannah River National Laboratory
Aiken, SC, USA

Dr. Bruce Hardy
Savannah River National Laboratory
Aiken, SC, USA

Dr. Martin Sulic
Savannah River Consulting
Aiken, SC, USA

Mr. Matthew Kesterson
Savannah River National Laboratory
Aiken, SC, USA

Dr. Claudio Corgnale
Savannah River Consulting
Aiken, SC, USA

Dr. Donald Anton
Savannah River National Laboratory
Aiken, SC, USA

ABSTRACT

Numerical models for the evaluation of cryo-adsorbent based hydrogen storage systems for fuel cell vehicles were developed and validated against experimental data. These models simultaneously solve the equations for the adsorbent thermodynamics together with the conservation equations for heat, mass, and momentum. The models also use real gas thermodynamic properties for hydrogen. Model predictions were compared to data for charging and discharging both activated carbon and MOF-5™ systems. Applications of the model include detailed finite element analysis simulations and full vehicle-level system analyses. The present work provides an overview of the compacted adsorbent storage prototype system, as well as a detailed computational analysis and its validation using 2-liter prototype test system. The results of these computational and experimental analyses are then projected to a full scale vehicle system, based on an 80 KW fuel cell with a 20 kW battery.

This work is part of the Hydrogen Storage Engineering Center of Excellence (HSECoE), which brings materials development and hydrogen storage technology efforts address onboard hydrogen storage in light duty vehicle applications. The HSECoE spans the design space of the vehicle requirements, balance of plant requirements, storage system components, and materials engineering. Theoretical, computational, and experimental efforts are combined to evaluate, design, analyze, and scale potential hydrogen storage systems and their supporting components against the Department of Energy (DOE) 2020 and Ultimate Technical Targets for Hydrogen Storage Systems for Light Duty Vehicles.

INTRODUCTION

The US DOE has been working with American automakers to overcome the technical and economic barriers associated hydrogen (H_2) fuel cell (FC) vehicles. One of the major technical barriers is onboard H_2 storage; the DOE has published a set of technical targets for H_2 vehicles to make them competitive with modern internal combustion engine (ICE) vehicles [1]. A summary table of these targets is provided in Annex A below. Several technologies, including compressed gas, cryo-compressed, and liquified hydrogen storage [2, 3], have shown great promise in fuel cell vehicles. Media-based hydrogen storage is also being examined and can be separated into three general categories: chemical hydrides [4, 5, 6], which must be refueled off-board; metal hydrides [7, 8, 9], that can be refueled on-board and are regenerated through a chemical reaction; and adsorbents [10, 11, 12, 13, 14], which store hydrogen via physisorption. The present paper focuses on hydrogen adsorption.

In an effort to bring materials development and hydrogen storage technologies together, the DOE formed the HSECoE. The HSECoE examined all three categories of media-based hydrogen storage. With respect to adsorbents, the HSECoE sought to create predictive adsorbent hydrogen storage computational models that have been validated experimentally by both excess adsorption measurements and laboratory-scale prototype adsorbent system evaluation. Hardy *et al.* [14] created hydrogen adsorption computational models for the HSECoE, which formed the basis for the adsorbent storage system design parametric study [15] and have been included in the HSECoE's full-scale vehicle framework model [16, 17]. Both the vehicle framework and the stand-alone design tool used in the parametric studies are available for download from the HSECoE's webpage (www.hsecoe.org).

The present work uses these validated adsorbent computational models within the FEA tool COMSOL® to analyze a hydrogen storage system comprised of an adsorbent and a heat exchanger within a pressure vessel. The hydrogen storage system shown here is based on the Modular Adsorbent Tank Insert (MATI) design, which was one of the two final adsorbent system designs within the HSECoE as described in a previous work [15] about the parametric analysis performed of possible adsorbent hydrogen storage systems.

NOMENCLATURE

BOP	Balance of Plant
DOE	Department of Energy
EERE	Energy Efficiency and Renewable Energy

FC	Fuel cell
FEA	Finite element analysis
H_2	Hydrogen
$H_{2,\ usable}$	Hydrogen gas that is used to move the FC vehicle (excluding heating/cooling systems, tank heel, etc.)
HSECoE	Hydrogen Storage Engineering Center of Excellence
ICE	Internal combustion engine
LN_2	Liquid nitrogen
m	Distribution parameter, set equal to 2
MOF	Metal organic framework
n_a	Absolute adsorption per unit mass of adsorbent [mol/kg]
n_{ex}	Excess adsorption per unit mass of adsorbent [mol/kg]
n_{max}	Limiting adsorption per unit mass of adsorbent [mol/kg]
n_{tot}	Total amount of gas stored within the system volume [mol]
P	Equilibrium pressure [Pa]
P_0	Pseudo-saturation pressure (within the adsorption model) [Pa]
R	Universal gas constant [8.314 J/mol-K]
SRC	Savannah River Consulting
SRNL	Savannah River National Laboratory
T	Equilibrium temperature [K]
US	United States
V_a	Adsorption volume per unit mass of adsorption [m^3/kg]
V_g	Interstitial volume within the adsorbent per unit mass of adsorbent [m^3/kg]
V_v	Void volume of the adsorption per unit mass of adsorption [m^3/kg]
α	Enthalpic contribution to the characteristic free energy of adsorption [J/mol]
B	Entropic contribution to the characteristic free energy of adsorption [J/mol-K]
ε	Characteristic free energy of adsorption ($\varepsilon = \alpha + \beta T$) [J/mol]
ρ_g	Density of the bulk gas in equilibrium with the adsorbed phase [mol/m^3]

ADSORBENT COMPUTATIONAL MODEL

The equations used to describe hydrogen adsorption are outlined in a previous work [15], but are summarized here for reference. The adsorption theory describing the process of hydrogen physisorption serves as the backbone of the adsorption-based calculations. The current work uses the Dubinin-Astakhov (D-A) model as outlined by Richard *et al.* [10, 11] to describe the hydrogen adsorption isotherms. The absolute adsorption (n_a) is given by the following equation:

$$n_a = n_{ex} + \rho_g V_a \quad (1)$$

where n_{ex} is the excess adsorption, ρ_g is the bulk gas density, and V_a is the adsorption volume. The adsorption volume is the volume of gas associated with the adsorption sites. There is also a void space (or void volume, V_v) within the adsorbent that is understood as all space within the adsorbent where gas could be. The void volume (V_v) is experimentally measured by helium probing or calculated from the adsorbent's bulk and skeletal densities. Within the adsorbent there is also interstitial space (or gas volume, V_g) where adsorption is negligible and the density of the gas is the same as the bulk gas. The relationship between these three volumes is given by the following equation:

$$V_g = V_v - V_a \quad (2)$$

The D-A model defines absolute adsorption as:

$$n_a = n_{max} \exp\left[-\left[\frac{RT}{\varepsilon}\right]^m \ln^m\left(\frac{P_0}{P}\right)\right] \quad (3)$$

where n_{max}, ε, and P_0 must be determined for the pressure and temperature range of interest. The exponent m was set to 2 for computational expediency, which is a special case of the D-A model corresponding to the Dubinin-Radushkevich equation.

Czerny *et al.* [12] provided the following equation for the characteristic free energy of adsorption:

$$\varepsilon = \alpha + \beta T \quad (4)$$

where α and β are the enthalpic and the entropic factors, respectively.

Combining equations 1-4 provides the following equation for excess adsorption:

$$n_{ex} = n_{max} \exp\left[-\left[\frac{RT}{\alpha+\beta T}\right]^2 \ln^2\left(\frac{P_0}{P}\right)\right] - \rho_g V_a \quad (5)$$

where n_{max}, α, β, P_0, and V_a are the fitting parameters used to match experimental isotherm data. The experimental isotherm data can also be used to calculate the isosteric heat of adsorption ($-\Delta\overline{h_a^0}$) according to the following equation provided by Myers and Monson [18]:

$$\Delta\overline{h_a^0} = -RT^2\left[\frac{\partial \ln P}{\partial T}\right]_{n_a,V} = -\alpha\sqrt{-ln\left(\frac{n_a}{n_{max}}\right)} \qquad (6)$$

This non-constant heat of adsorption is used within the energy balance equation to account for the changes in temperature within hydrogen adsorption/desorption.

ADSORBENT SYSTEM DESIGN

With help from US auto manufacturers, the DOE EERE created a list of technical targets for onboard hydrogen storage systems to ensure that these vehicles could compete with internal combustion engine vehicles [1]. The HSECoE ranked these technical targets and concluded that the three most important results were the estimate system cost, volumetric capacity ($H_{2,usable}$ mass / total system volume), and gravimetric capacity ($H_{2,usable}$ mass / total system mass), in that order. Note that these technical targets are based on the total storage system design, including the hydrogen storage material, pressure vessel, heat exchanger, and any other balance of plant (BOP) components that may be necessary to implement the system on a vehicle. Schematics of full adsorbent-based hydrogen storage systems were shown by Tamburello *et al*. [15]

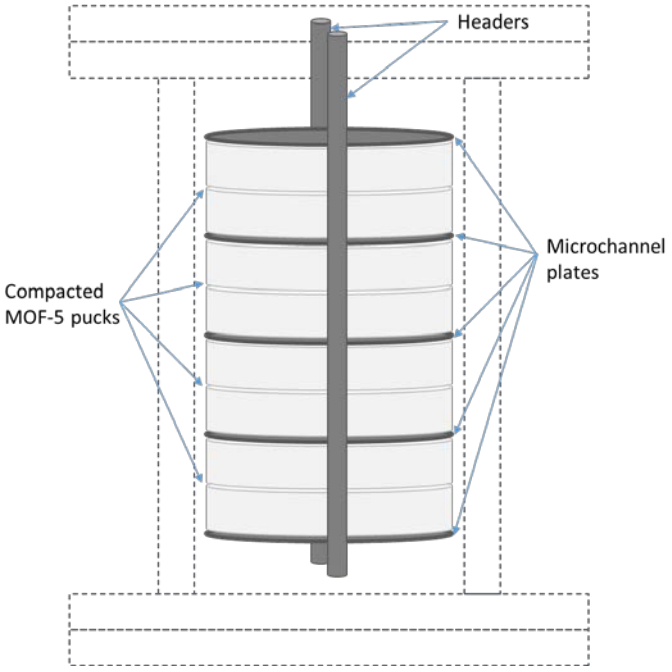

Figure 1. Schematic [15] of the MATI internal heat exchanger within the HSECoE's 2-liter prototype pressure vessel.

Powder adsorbents, such as activated carbon and metal organic frameworks (MOFs), have difficulty meeting the volumetric capacity technical target. For this reason, mechanical compaction has been used to form pucks in an effort to increase the volumetric capacity [18, 19, 20]. While this has helped, it has also created problems when trying to package and/or thermally control the adsorbent pucks. The HSECoE examined several heat exchanger designs that could address these shortcomings, with the MATI heat exchangers showing the most promise [15]. The dissertation by Loeb at Oregon State University [21] provides a good explanation of the MATI, its development, and its capabilities. The MATI isolated-fluid heat exchanger design offers several benefits, including:

- Microchannel plates designed to transfer the fluid temperature to the adsorbent *instantly*.
- Unit cell design ensures that the temperature profiles for each plate are *identical*.
- Designed to withstand pressures > 100 bar outside of the heat exchanger and LN_2 boiling within.
- Minimal volume and mass needed.

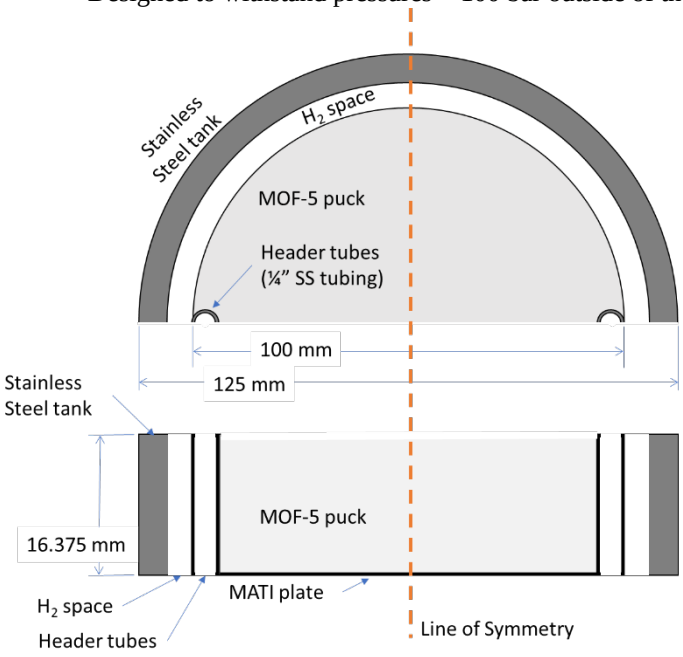

Figure 2. Sketch of the half MATI unit cell geometry from the HSECoE's 2-liter prototype.

These capabilities have been confirmed experimentally using a 2-liter prototype designed around the MATI heat exchanger and compacted MOF-5™ pucks, but this is beyond the scope of the current paper and will be published in a future work. A basic schematic of the MATI heat exchanger within the 2-liter prototype is shown in Figure 1 (reproduced from reference [15]).

A computational model of a MATI heat changer unit cell with a MOF-5™ puck compacted to 0.4 g/cc to match the HSECoE's 2-liter prototype was created in COMSOL®. Figures 2 and 3 show a basic sketch of the half-unit cell geometry and the quarter unit cell COMSOL® geometry with its boundary conditions and material sections, respectively. Note that the model takes advantage of several symmetries within the MATI's unit cell to minimize the geometry necessary to get an accurate representation of the HSECoE's 2-liter prototype. One such symmetry (denoted by the *line of symmetry* in Figure 2) is made possible by the uniform temperature measured experimentally across the MATI plates as LN2 is flowed through them. These experimental measurements are beyond the scope of the current paper and will be published in a future work.

COMSOL Multiphysics® is a general-purpose FEA software platform for modeling engineering applications. The software platform allows the users to define geometries, material properties,

and the physics that describe specific phenomena through the core Multiphysics® package and add-on modules for specific engineering applications, such as fluid flow, heat transfer, and chemical engineering. For the current work, the heat transfer and fluid flow modules were utilized to access the *Heat Transfer in Porous Media* and *Brinkman Equation* physics packages, respectively. The model is broken into three material sections—adsorbent, hydrogen gas, and stainless-steel—as shown in Figure 3.

Using equations 5 and 6 above, the adsorbent generates hydrogen and heat, respectively, based on the bulk temperature and pressure and the D-A parameters for compacted MOF-5™ (as listed in Table 1) as hydrogen is adsorbed. Based on empirical data from work done by the HSECoE, the thermal conductivity was set to 0.3 W/m-K. In addition, the specific heat was experimentally shown to be within 10% of activated carbon. The final two parameters of note are the porosity and the permeability of the compacted pucks, which were set to 12.66% and 2e-13 m^2, respectively. Many of these material properties may vary from those found within the literature, but this can be attributed to the source and condition of the adsorbent versus what was used by the HSECoE.

Table 1. D-A parameters for 0.4 g/cc compacted MOF-5™

Parameter	Units	Value
ρ_{ads}	[kg/m^3]	406
α	[J/mol]	2541.5
β	[J/mol/K]	8.0691
n_{max}	[mol/kg]	70.178
P_0	[Pa]	1.9273e8
V_a	[m^3/kg]	0.0016382
V_v	[m^3/kg]	0.0019500

COMPUTATIONAL MODEL RESULTS

The computational model results are broken into three sections: validation, refueling, and driving. For each scenario, the unit cell model matching the HSECoE's 2-liter prototype was run to provide additional insight beyond the prototype experiments (to be shown in a future publication) and the system model analyses (from reference [15]).

Model Validation

To validate the computational model, the 2-liter prototype was refueled from 1 bar to 100 bar at constant temperature (submerged in a LN_2 bath). The pressure was ramped over 14 minutes to minimize the heat of pressurization within the 2-liter pressure vessel during refueling. Even with insulation, stainless-steel tubing was exposed to ambient outside of the LN_2 bath and, thus, the constant temperature boundary condition was experimentally measured to be approximately 83 K at the outer pressure vessel wall. In addition, the MATI plates were shown to match near-LN_2 temperatures within seconds of the LN_2 flow within the MATI microchannels and, thus, a constant temperature boundary condition was used within the MATI plates as well. Note that 83 K was measured at the MATI plates as well and can also be attributed to heat transfer from insulated tubing exposed to the ambient.

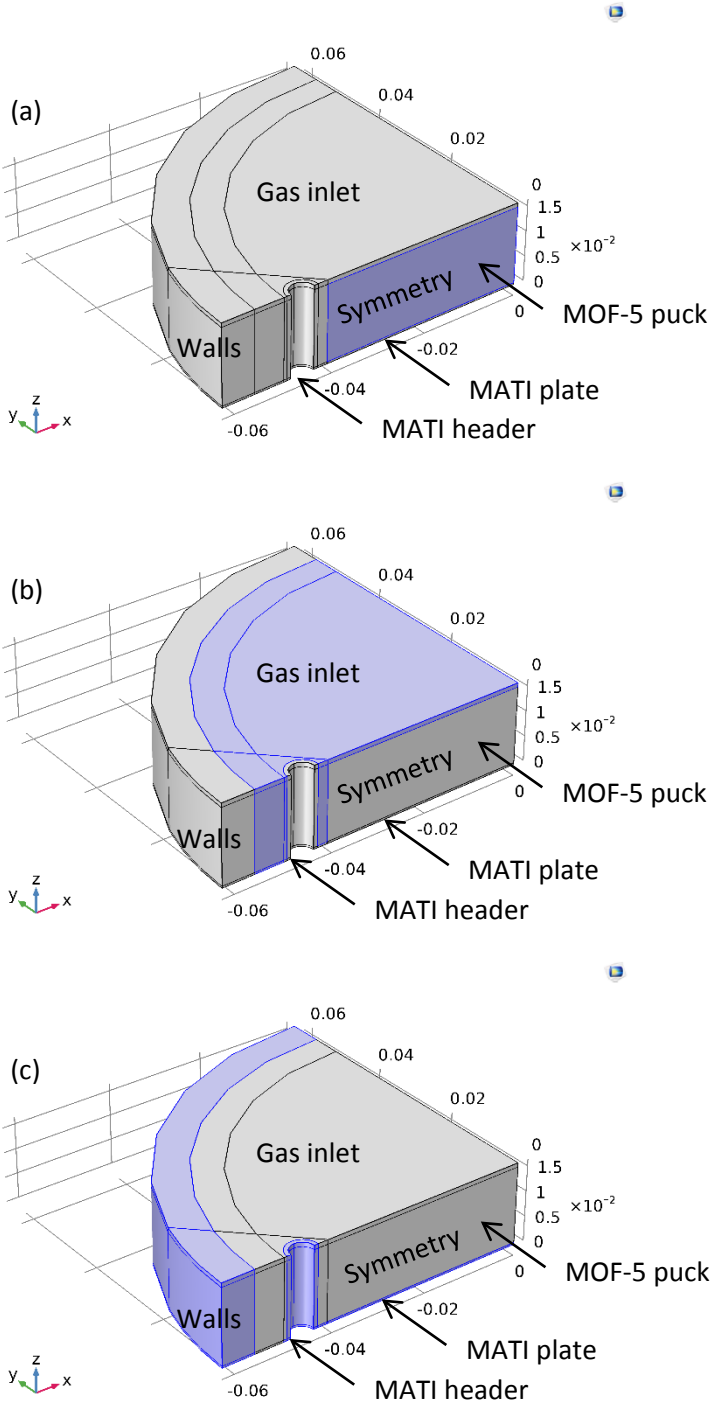

Figure 3. COMSOL® geometry and boundary conditions of the quarter MATI unit cell. Sections: (a) adsorbent, (b) hydrogen gas, and (c) stainless-steel.

The schematic in Figure 1 shows a 5-plate MATI assembly like the one used in the 2-liter prototype experiments. Note that plate #1 is near the top closest to the tubing inlet/outlet and plate #5 is near the bottom farthest from the tubing inlet/outlet. Temperature profiles for both the constant temperature refueling experiment and its computational model at the center of the MOF-5^{TM} pucks are shown in Figure 4. The experimental profiles show that the adsorbent pucks near plate #1 (closest to the inlet/outlet tubing) reach the highest temperatures and take the largest amount of time to reach equilibrium pressure after refueling (beyond the data shown in Figure 4). The temperature profiles for the subsequent plates decrease in maximum temperature and the time necessary to reach equilibrium until plate #5, which is farthest from the tubing inlet/outlet.

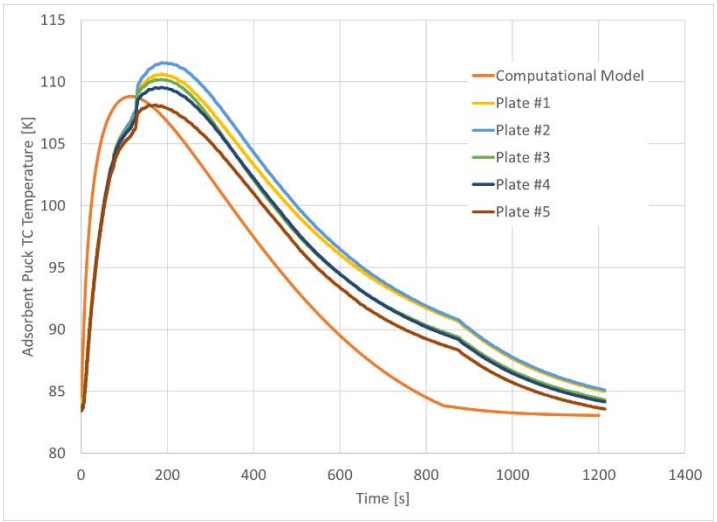

Figure 4. Temperature profiles of constant temperature refueling from 1 bar to 100 bar.

The temperature profile for the computational model at the puck center shows good agreement with the experiment overall, but with several differences. The computational model reaches its maximum temperature sooner than the experiment, which can be attributed to the ideal boundary conditions in the model. The computational model also reaches a lower maximum temperature and reaches equilibrium more quickly than the experiment, which can be attributed to the heat of pressurization that was minimized in the model versus the experiment.

5-minute Refueling

For the 5-minute refueling simulation, the model is initialized to 25°C and 1 bar. The pressure is increased to 100 bar over 5 seconds while the MATI plate boundary temperature is dropped to 77 K over 10 seconds. Note that because the boundary conditions ramped so quickly, the results from this simulation can be used for a 3 minute or 5 minute refueling event, as each is of interest to the DOE. To mimic a full-scale hydrogen storage system that would be wrapped in multi-layer vacuum insulation, an insulation boundary condition is implemented on the outer walls of the stainless-steel pressure vessel.

Figures 5 and 6 show profiles for the average MOF-5 puck temperature and the hydrogen refueling, respectively. As the pressure increases over the first few seconds, the average puck temperature increases due to the heat of adsorption and heat of pressurization. In addition, the rate of hydrogen refueling (and the resulting amount of H_2 stored) increases dramatically over the first 20 seconds. After the initial 20 seconds, the rate of hydrogen refueling levels off and then decreases steadily as the number of available adsorption sites decreases. Similarly, the average puck temperature decreases until the entire puck approaches the MATI plate temperature. Figure 7 provides temperature distributions throughout the unit cell model at several times during refueling. Note that the temperature scale changes for each distribution to better show the gradient at each time. The adsorbent is slow to change in temperature due to its poor thermal conductivity, which is common for adsorbents.

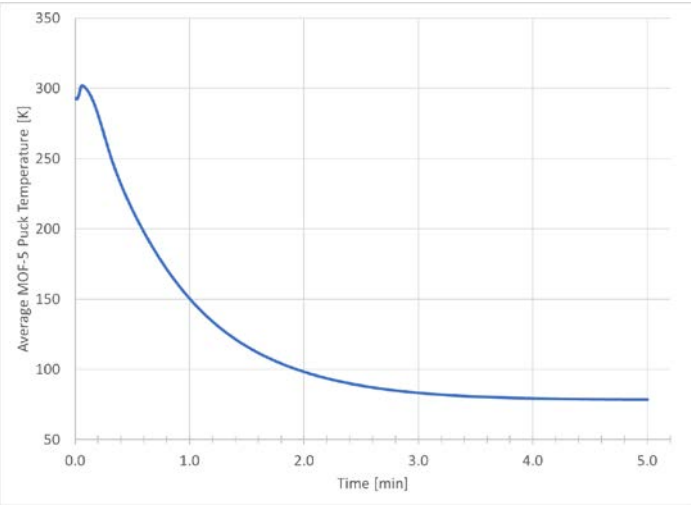

Figure 5. Average puck temperature profile during 5-minute refueling.

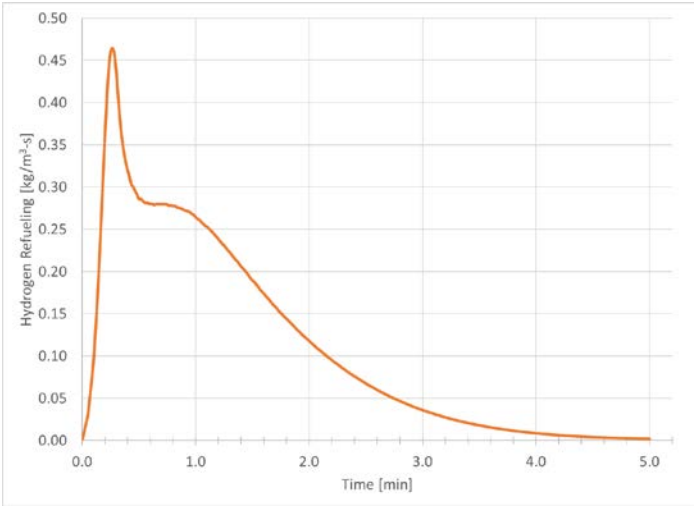

Figure 6. Hydrogen refueling rate during 5-minute refueling.

Constant Driving

A driving scenario was then examined by initializing the system to 80 K and 100 bar and imposing a constant hydrogen draw rate of 86 μm/s at the gas inlet. To control the hydrogen release from the adsorbent, pressure is used to drive the hydrogen to the fuel cell while temperature is used to maintain the pressure as necessary. A hold pressure of roughly 20 bar is used to ensure that there is significant pressure to supply the fuel cell during an acceleration event. As the pressure approaches the hold pressure, the MATI plate boundary temperature is increased until the maximum average puck temperature is reached (at which point the system pressure can drop to the minimum pressure needed to supply the fuel cell). This temperature and pressure behavior is shown in Figure 8, which provides the average MOF-5™ puck temperature and pressure during driving. Note that an insulation boundary condition is imposed on the outer wall of the stainless-steel pressure vessel.

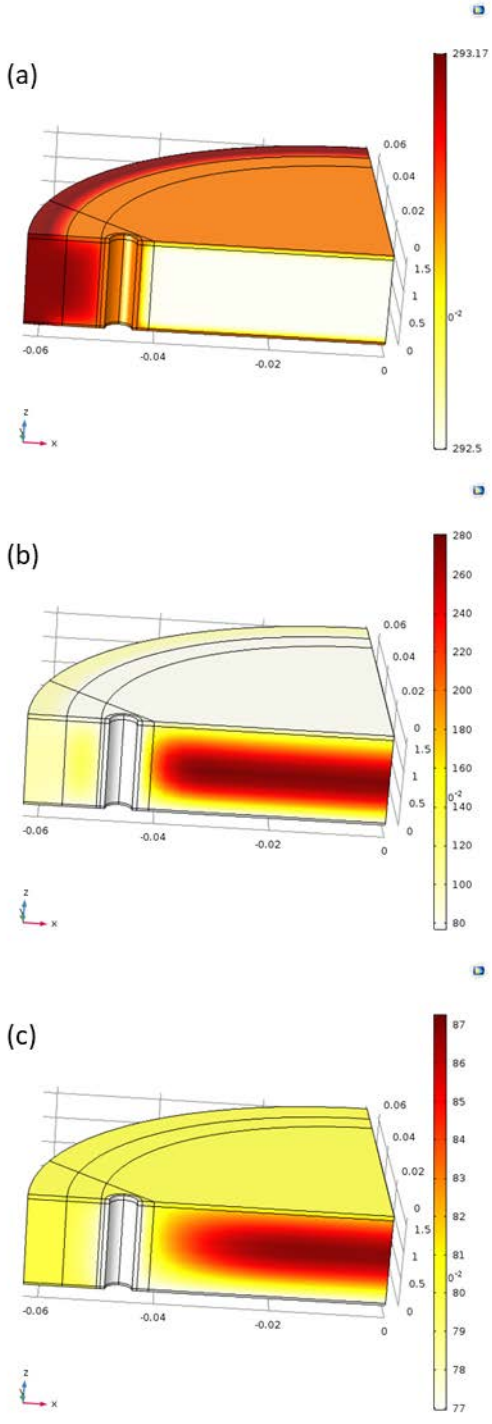

Figure 7. Temperature profiles at (a) 1 second, (b) 30 seconds, and (c) 180 seconds during a 5-minute refueling.

Figure 9 shows temperature distributions through the unit cell model at several times during driving. As previously noted with Figure 7, the temperature scale changes for each distribution to better show the temperature gradient at each time. Unlike during refueling, the temperature distributions are more even during driving because the there is a greater amount of time available to transfer the heat throughout the adsorbent, even with the poor thermal conductivity of most adsorbents. As expected, the adsorbent temperature is highest near the MATI plate and lowest near the hydrogen gas toward the stainless-steel pressure vessel wall within the LN_2 bath.

CONCLUSIONS AND FUTURE WORK

COMSOL Multiphysics® was used to analyze a hydrogen storage system comprised of an adsorbent and a heat exchanger within a pressure vessel. This system was validated against experimental results 2-liter prototype and used to show adsorbent behavior during refueling and driving. The hydrogen storage system shown here is based on the Modular Adsorbent Tank Insert (MATI) design, which was one of the two final adsorbent system designs within the HSECoE as described in a previous work [15] about the parametric analysis performed of possible adsorbent hydrogen storage systems. While this validated computational model was used to analyze a unit cell representation of the HSECoE's 2-liter prototype, this model can be extended to other adsorbents, heat

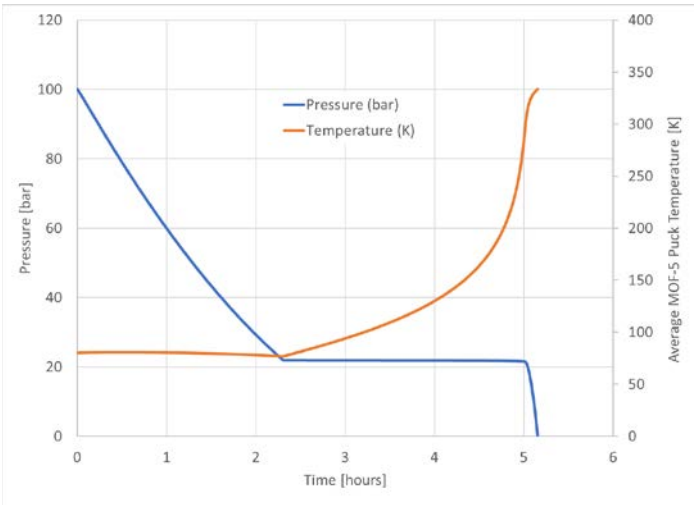

Figure 8. Temperature and pressure controls during the drive cycle.

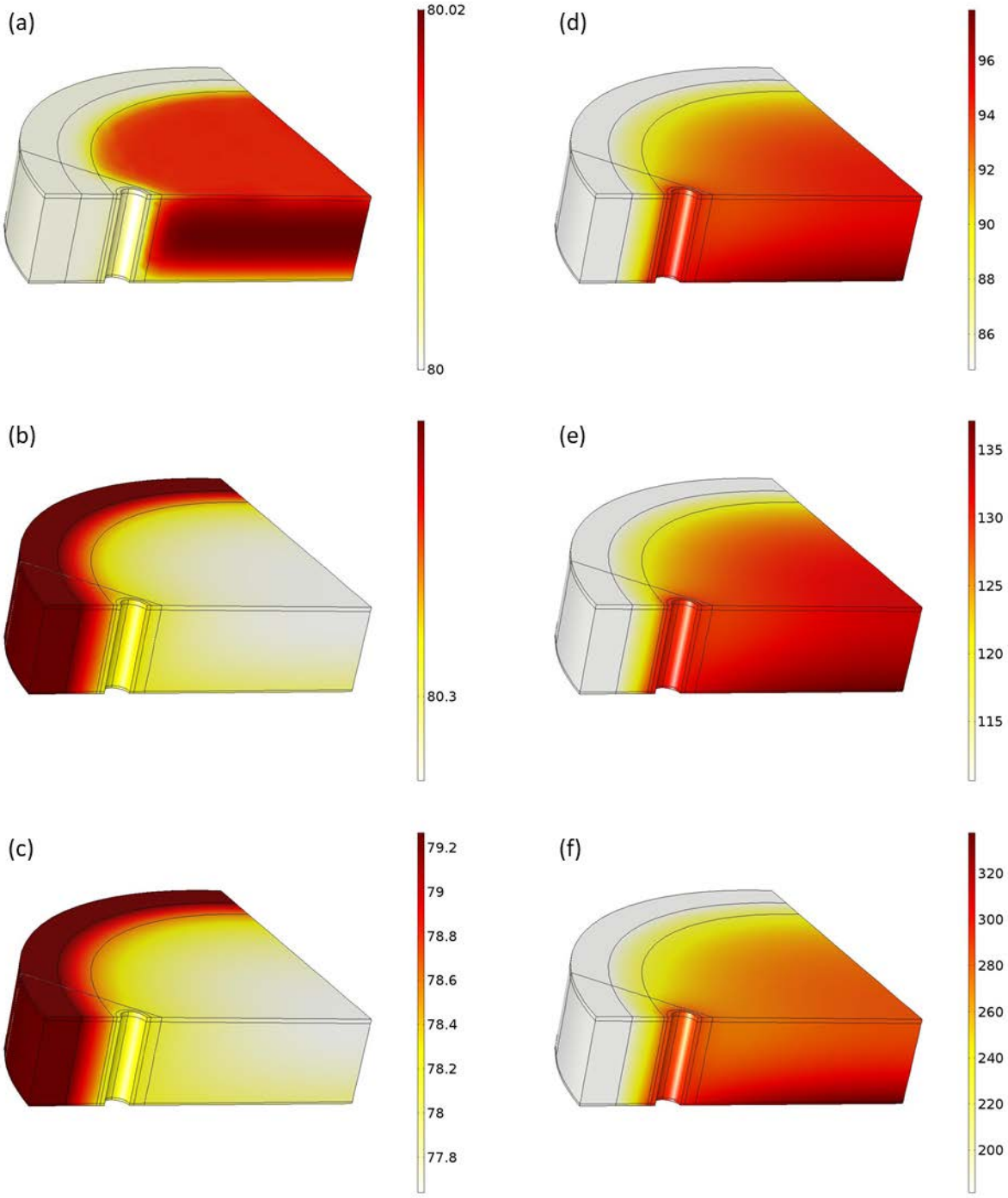

Figure 9. Temperature profiles at (a) 20 seconds, (b) 1 hour, (c) 2 hours, (d) 3 hours, (e) 4 hours, and (f) 5 hours during driving.

exchangers, and/or system designs as needed. As new materials and hydrogen storage systems are discovered/designed, this model can be used to better understand them.

ACKNOWLEDGMENTS

This document was prepared in conjunction with work accomplished for the Fuel Cell Technologies Office within the US DOE's EERE as part of the HSECoE.

DISCLAIMER

The views and opinions of the authors expressed herein do not necessarily state or reflect those of the United States Government or any agency thereof. Neither the United States Government nor any agency thereof, nor any of their employees, makes any warranty, expressed or implied, or assumes any legal liability or responsibility for the accuracy, completeness, or usefulness of any information, apparatus, product, or process disclosed, or represents that its use would not infringe privately owned rights.

REFERENCES

[1] https://energy.gov/eere/fuelcells/doe-technical-targets-onboard-hydrogen-storage-light-duty-vehicles.

[2] Satyapal, S., Petrovic, J., Read, C., Thomas, G., and Ordaz, G., (2007), "The U.S. Department of Energy's National Hydrogen Storage Project: Progress towards meeting hydrogen-powered vehicle requirements." *Catalysis Today* **120**, 246-256.

[3] Ahluwalia, R.K., Hua, T.Q., Peng, J.-K., Lasher, S., McKenney, K., Sinha, J., and Gardiner, M., (2010), "Technical assessment of cryo-compressed hydrogen storage tank systems for automotive applications." *Int. J. Hydrogen Energy* **35**, 4171-4184.

[4] Hardy, B.J. and Anton, D.L., (2009), "Hierarchical methodology for modeling hydrogen storage systems. Part I: Scoping models." *Int. J. Hydrogen Energy* **34**, 2269-2277.

[5] Hardy, B.J. and Anton, D.L., (2009), "Hierarchical methodology for modeling hydrogen storage systems. Part II: Detailed models." *Int. J. Hydrogen Energy* **34**, 2992-3004.

[6] Garrison, S.L., Hardy, B.J., Gorbounov, M.B., Tamburello, D.A., Corgnale, C., van Hassel, B.A., Mosher, D.A., and Anton, D.L., (2012), "Optimization of internal heat exchangers for hydrogen storage tanks utilizing metal hydrides." *Int. J. Hydrogen Energy* **37**, 2850-2861.

[7] Mohan, G., Prakash Maiya, M., and Srinivasa Murthy, S., (2007), "Performance simulation of metal hydride hydrogen storage device with embedded filters and heat exchanger tubes." *Int. J. Hydrogen Energy* **32**, 4978-4987.

[8] Botzung, M., Chaudourne, S., Gillia, O., Perret, C., Latroche, M., Percheron-Guegan, A., and Marty, P., (2008), "Simulation and experimental validation of a hydrogen storage tank with metal hydride." *Int. J. Hydrogen Energy* **33**, 98-104.

[9] Raju, M., Ortmann, J.P., and Kumar, S., (2010), "System simulation model for high-pressure metal hydride hydrogen storage systems." *Int. J. Hydrogen Energy* **35**, 8742-8754.

[10] Richard, M.-A., Benard, P., and Chahine, R., (2009), "Gas adsorption process in activated carbon over a wide temperature range above the critical point. Part 1: modified Dubinin-Astakhov model." *Adsorption* **15**, 43-51.

[11] Richard, M.-A., Benard, P., and Chahine, R., (2009), "Gas adsorption process in activated carbon over a wide temperature range above the critical point. Part 2: conservation of mass and energy", *Adsorption* **15**, 53-63.

[12] Czerny, A.M., Benard, P., and Chahine, R., (2005), "Adsorption of nitrogen on granular activated carbon: experiment and modeling." *Langmuir* **21**, 2871-2875.

[13] Zhou, W., Wu, H., Hartman, M.R., and Yildirim, T., (2007), "Hydrogen and methane adsorption in metal-organic frameworks: A high-pressure volumetric study." *J. Phys. Chem. C* **111**, 16131-16137.

[14] Hardy, B.J., Corgnale, C., Chahine, R., Richard, M.-A., Garrison, S., Tamburello, D., Cossement, D., and Anton, D., (2012), "Modeling of adsorbent based hydrogen storage systems." *Int. J. of Hydrogen Energy* **37**, 5691-5705.

[15] Tamburello, D.A., Hardy, B.J., Corgnale, C., Sulic, M., and Anton, D.L., (2017), "Cryo-adsorbent hydrogen storage systems for fuel cell vehicles." *Proceedings of the ASME 2017 Fluids Engineering Division Summer Meeting*, **FEDSM2017-69411**.

[16] Pasini, J.-M., van Hassel, B.A., Mosher, D.A., and Veenstra, M.J., (2012), "System modeling methodology and analysis for materials-based hydrogen storage." *Int. J. Hydrogen Energy* **37**, 2874-2884.

[17] Thornton, M., Brooker, A., Cosgrove, J., Veenstra, M., and Pasini, J.M., (2012), "Development of a vehicle-level simulation model for evaluating the trade-off between various advanced on-board hydrogen storage technologies for fuel cell vehicles." *SAE Technical Paper* **2012-01-1227**.

[18] Xu, C., Yang, J., Veenstra, M., Sudik, A., Purewal, J.J., Ming, Y., Hardy, B.J., Warner, J., Maurer, U., and Siegel, D.J., (2013), "Hydrogen permeation and diffusion in densified MOF-5 pellets." *Int. J. Hydrogen Energy* **38** (8), 3268-3274.

[19] Purewal, J.J., Liu, D., Yang, J., Sudik, A., Siegel, D.J., Maurer, S., and Muller, U., (2012), "Increased volumetric hydrogen uptake of MOF-5 by powder densification." *Int. J. Hydrogen Energy* **37**, 2723-2727.

[20] Liu, D., Purewal, J.J., Yang, J., Sudik, A., Maurer, S., Mueller, U., Ni, J., and Siegel, D.J., (2012), "MOF-5 composites exhibiting improved thermal conductivity." *Int. J. Hydrogen Energy* **37**, 6109-6117.

[21] Loeb, C.S., (2013), "Enhancement and modeling of cryogenic solid-state hydrogen storage systems with a novel microchannel thermal management device." *http://ir.library.oregonstate.edu/concern/graduate_thesis_or_dissertations/5t34sq07x*.

ANNEX A

DOE EERE ONBOARD HYDROGEN STORAGE TECHNICAL TARGETS [1]

Technical System Targets: Onboard Hydrogen Storage for Light-Duty Fuel Cell Vehicles [a] (updated May 2015)			
Storage Parameter	**Units**	**2020**	**Ultimate**
System Gravimetric Capacity: Usable, specific-energy from H_2 (net useful energy/max system mass) [b]	kWh/kg (kg H_2/kg system)	1.8 (0.055)	2.5 (0.075)
System Volumetric Capacity: Usable energy density from H_2 (net useful energy/max system volume) [b]	kWh/L (kg H_2/L system)	1.3 (0.040)	2.3 (0.070)
Storage System Cost : • Fuel cost [c]	$/kWh net ($/kg H_2) $/gge at pump	10 333 2-4	8 266 2-4
Durability/Operability: • Operating ambient temperature [d] • Min/max delivery temperature • Operational cycle life (1/4 tank to full) • Min delivery pressure from storage system • Max delivery pressure from storage system • Onboard Efficiency [e] • "Well" to Powerplant Efficiency [e]	 ºC ºC Cycles bar (abs) bar (abs) % %	 -40/60 (sun) -40/85 1500 5 12 90 60	 -40/60 (sun) -40/85 1500 5 12 90 60
Charging / Discharging Rates: • System fill time (5 kg) • Minimum full flow rate • Start time to full flow (20°C) • Start time to full flow (-20°C) • Transient response at operating temperature 10%–90% and 90%–0%	 min (kg H_2/min) (g/s)/kW s s s	 3.3 (1.5) 0.02 5 15 0.75	 2.5 (2.0) 0.02 5 15 0.75
Fuel Quality (H_2 from storage) [f]:	% H_2	SAE J2719 and ISO/PDTS 14687-2 (99.97% dry basis)	
Environmental Health & Safety: • Permeation & leakage [g] • Toxicity • Safety	 - - -	Meets or exceeds applicable standards	
Loss of useable H_2 [h]	(g/h)/kg H_2 stored	0.05	0.05

* Useful constants: 0.2778 kWh/MJ; Lower heating value for H_2 is 33.3 kWh/kg H_2; 1 kg H_2 ≈ 1 gal gasoline equivalent (gge)

Footnotes to Target Table:

[a] Targets are based on the lower heating value of hydrogen, 33.3 kWh/kg H_2. Targets are for a complete system, including tank, material, valves, regulators, piping, mounting brackets, insulation, added cooling capacity, and all other balance-of-plant components. All capacities are defined as useable capacities that could be delivered to the fuel cell power plant. All targets must be met at the end of service life (approximately 1500 cycles or 5000 operation hours, equivalent of 150,000 miles).

[b] Capacities are defined as the useable quantity of hydrogen deliverable to the powerplant divided by the total mass/volume of the complete storage system, including all stored hydrogen, media, reactants (e.g., water for hydrolysis-based systems), and system components. Capacities must be met at end of service life. Tank designs that are conformable and have the ability to be efficiently package onboard vehicles may be beneficial even if they do not meet the full volumetric capacity targets.